Experimental and theoretical investigations of the [Ln(β-dik) $(NO_3)_2(phen)_2]\cdot H_2O$ luminescent complexes

Paulo R.S. Santos, Dariston K.S. Pereira, Israel F. Costa, Iran F. Silva, Hermi F. Brito, Wagner M. Faustino, Albano N. Carneiro Neto, Renaldo T. Moura, Jr., Maria H. Araújo, Renata Diniz, Oscar L. Malta, Ercules E.S. Teotonio

PII: S0022-2313(20)30733-X

DOI: https://doi.org/10.1016/j.jlumin.2020.117455

Reference: LUMIN 117455

To appear in: *Journal of Luminescence*

Received Date: 8 April 2020

Revised Date: 18 May 2020

Accepted Date: 7 June 2020

Please cite this article as: P.R.S. Santos, D.K.S. Pereira, I.F. Costa, I.F. Silva, H.F. Brito, W.M. Faustino, A.N. Carneiro Neto, R.T. Moura Jr., M.H. Araújo, R. Diniz, O.L. Malta, E.E.S. Teotonio, Experimental and theoretical investigations of the [Ln(β-dik) $(NO_3)_2(phen)_2]\cdot H_2O$ luminescent complexes, *Journal of Luminescence* (2020), doi: https://doi.org/10.1016/j.jlumin.2020.117455.

Experimental and theoretical investigations of the [Ln(β-dik)$(NO_3)_2(phen)_2]\cdot H_2O$ luminescent complexes

Paulo R. S. Santos[1], Dariston K. S. Pereira[1], Israel F. Costa[1], Iran F. Silva[1], Hermi F. Brito[2], Wagner M. Faustino[1], Albano N. Carneiro Neto[3], Renaldo T. Moura Jr.[4], Maria H. Araújo[5], Renata Diniz[5], Oscar L. Malta[6], Ercules E. S. Teotonio[1,*]

[1] Department of Chemistry, Federal University of Paraíba, João Pessoa, Brazil

[2] Institute of Chemistry, Department of Chemistry, University of São Paulo, São Paulo, Brazil

[3] Physics Department and CICECO – Aveiro Institute of Materials, University of Aveiro, Aveiro, Portugal

[4] Department of Chemistry and Physics, Federal University of Paraíba, Areia, Brazil

[5] Departament of Chemistry, ICEx, University of Minas Gerais, Belo Horizonte, MG 31270-901, Brazil

[6] Department of Fundamental Chemistry, Federal University of Pernambuco, Recife, Brazil

*Corresponding author: email: teotonioees@quimica.ufpb.br

Phone: +55-83-3216-7591

Abstract

In this work, the coordination compounds presenting the formulas $[Eu(acac)(NO_3)_2(phen)_2]\cdot H_2O$ (**Eu1**) and $[Eu(bzac)(NO_3)_2(phen)_2]\cdot H_2O$ (**Eu2**), acac: acetylacetonate, bzac: benzoylacetonate and, phen: 1,10-phenantroline, were successfully synthesized and some spectroscopic properties were investigated by theoretical and experimental methods. These compounds were characterized via elemental analysis, FTIR spectroscopy and thermogravimetric analysis (TGA). The X-ray diffraction data revealed that the compound **Eu1** crystallizes in the monoclinic space group P2/n. Spectroscopic data showed that ligand-to-metal charge transfer states (LMCT) in the $[Eu(\beta\text{-dik})(NO_3)_2(phen)_2]\cdot H_2O$ complexes (β-dik: acac or bzac) are redshift as compared with $[Eu(\beta\text{-dik})_3(phen)]$ complexes. These data showed that LMCT states play the most important role on the luminescence quenching in the complexes **Eu1** and **Eu2**, which only exhibit high luminescence intensities at low temperatures. Furthermore, the role of changes in the chemical environment on the intensity parameters Ω_λ (λ = 2 and 4) have been investigated from the theoretical point of view for the complexes **Eu1** to **Eu2**, and from these to tris β–dik complexes. Interestingly, the theoretical intensity parameters ration Ω_2/Ω_4 calculated are in a good agreement with those experimental ones.

Graphical Abstract

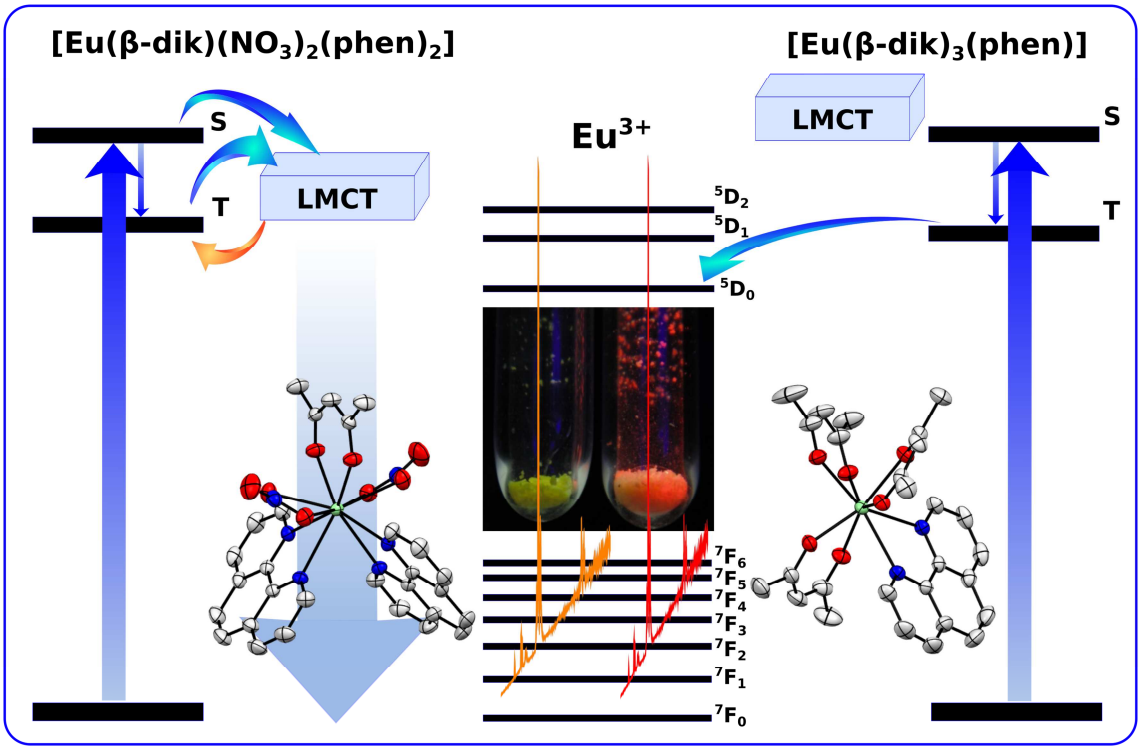

Highlights

- Europium(III) β-diketonate complexes were successfully synthesized.
- LMCT states play an essential role on the luminescent properties of Eu^{3+} complexes.
- The intensity parameters highly dependent on geometry and coordination number.

1. Introduction

Luminescent europium tetrakis- and tris-(β-diketonate) complexes have been receiving considerable attention since they are promising materials for application in lighting and electronic devices, [1,2] temperature and chemical sensors [3,4] and biomarkers [5] applications. The characteristic emissions emerging from these materials are due to the intraconfigurational $^5D_0 \rightarrow {}^7F_J$ (J = 0-6) transitions centered in the Eu^{3+} ion. Although the lanthanide ions have the low molar absorption coefficients ($\varepsilon \cong 1.0$ L·mol^{-1}·cm^{-1}), a high-intensity red luminescence can be obtained by indirect excitation from the β-diketonate ligands, which absorb photons and transfer energy efficiently to the lanthanide ion. In this context, designing highly luminescent materials based on the Ln^{3+} complexes often involves fine-tuning of excited ligand states in order to optimize the ligand-to-metal energy transfer and minimize non-radiative processes via multiphonon relaxation or ligand-to-metal charge transfer state (LMCT) [6,7].

Among europium tris-(β-diketonate) complexes, those containing neutral ligands (such as phosphine oxides, heteroaromatic amines and amides) have received special attention from both theoretical and experimental viewpoints [6,8,9]. In particular, the complexes with the general formula [Eu(β-dik)$_3$L], where L is 1,10-phenanthroline or 2,2'-bipyridine ligand, have been extensively studied due to these bidentate neutral ligands lead in the formation, leading to the luminescence europium compounds [10]. The high luminescence intensity of these complexes suggests that LMCT states are not acting as efficiently luminescence quenching channels. Furthermore, due to their molecular planarity, substantial inter or intramolecular π-π stacking interactions may result in unusual crystal structures [11,12].

Despite the growing interest of intramolecular ligand-to-metal energy transfer in this kind of complexes, there have been only a few detailed studies reporting on the spectroscopic properties of the europium mixed ligand complexes that present only one β-diketonate ligand coordinated. Previous reports had been concerned mainly on the structural and luminescent properties of Tb^{3+} complexes [13–15]. Moreover, no theoretical or experimental investigations have focused on the role of the LMCT state in the quarternary or quinternary mixed ligand complexes, except by our research group on the luminescent properties of the [Eu(dpm)$_2$(NO$_3$)(tppo)$_2$] complexes [16]. In this study, we have focused on the spectroscopic properties unusual complexes of general formula [Eu(β-

dik)$(NO_3)_2(phen)_2$], where β-dik = acetylacetonate (acac) or benzoylacetonate (bzac) ligands, taking into account the role of the ligand-to-metal charge transfer (LMCT) state on the photoluminescent properties of this kind of system. Furthermore, synthesis and characterization, including single-crystal X-ray diffraction of the [Eu(acac)$(NO_3)_2(phen)_2$] complex and thermogravimetric analysis will be discussed. It is found that low-energy LMCT state close to excited ligand states may effectively quench the Eu^{3+} luminescence in the [Eu(β-dik)$(NO_3)_2(phen)_2$] complexes. In sharp contrast, this luminescence quenching phenomenon is not operative in the [Eu(β-dik)$_3$(phen)] complexes. Furthermore, a theoretical study was performed to understand the role of the geometry transformation in these kind of complexes on the values of luminescence intensity parameters Ω_λ (λ =2 and 4). In this case, a scan calculations performing geometry transformations from **Eu1** and **Eu2** to [Eu(acac)$_3$(phen)] (**Eu3**) and [Eu(bzac)$_3$(phen)] (**Eu4)** were done using the SPARKLE/PM3 method [17] and the ratio Ω_2/Ω_4 were theoretically determined according to the Bond Overlap Model (BOM) [18] and Simple Overlap Model (SOM) [19] and compared with the experimental values [18,20–22].

2. Materials and methods

2.1. Chemical reagents and instruments

All reagents and solvents were of analytical grade and used without previous treatment: Ethanol (Tedia, 99.3%), methanol (Tedia, 99.8 %), nitric acid (Nuclear, 65.0%), europium oxide (Eu_2O_3) (Aldrich, 99.999%), gadolinium oxide (Gd_2O_3) (Alfa Aesar, 99.999%), acetylacetone (Merck, 99.8%), benzoylacetone (Aldrich, 99.8%), 1,10-phenantroline (Aldrich, 99.0%).

Microanalyses of carbon, hydrogen and nitrogen were performed on a Perkin Elmer 2400 series 2 Elemental Analysis Instrument. The europium and gadolinium amount in the complexes were determined using EDTA titration agent. Fourier Transform Infrared (FTIR) spectra were carried out using a spectrophotometer Shimadzu, model IRPrestige-21, by dispersing approximately 3 mg of the complexes in 100 mg of the KBr pallet. Thermogravimetric analyses (TGA) of the complexes in the temperature interval 30-800^{o}C were performed in a thermobalance DTG-60 Shimadzu, using approximately 8 mg of the sample in the platinum pan under an air flow rate of 50 mL·min^{-1} and a heating rate of 10

$^{o}C \cdot min^{-1}$. The diffuse reflectance spectra of the complexes were recorded in the spectral range from 190 to 1600 nm on a UV-3600 spectrophotometer, using an integrating sphere, model ISR-3100. For this analysis, the solid samples were distributed homogeneously over barium sulfate ($BaSO_4$), which was also used as a reflectance standard. A suitable single crystal of the $[Eu(acac)(NO_3)_2(phen)_2] \cdot H_2O$ compound for collecting X-ray diffraction measurement data was mounted on a SuperNova Rigaku diffractometer operating with Mo-K_α (λ = 0.71073 Å) radiation source at 293 K. The data collection, cell refinements, and intensity corrections for Lorentz and polarization effects were performed using CrysAlisPro software [23]. The structure of this compound was solved using SIR-2014 software [24] and refined by Full-matrix least-squares on F^2 using SHELXL-2018/3 [25] in WinGX program system [26]. The position and anisotropic atomic displacement parameters for all non-hydrogen atoms were refined, while hydrogen atoms positions were calculated with isotropic thermal parameters. The figures were drawn using Ortep-3 for windows [27] and Mercury [28] programs.

The luminescence measurements in the visible region were performed on a HORIBA Fluorolog-3 spectrofluorimeter, which consists of double SPEX 1692 monochromators with 1200 slots / mm (resolution 0.3 ± 0.5nm), a Xenon lamp excitation source 450 W and a R928P PMT photomultiplier as a detector. All measurements were made using the "front-face" frontal angle mode. Excitation spectra were recorded in the spectral range from 250 to 590 nm, while emission spectra from 550 to 730 nm, at liquid nitrogen temperature (77 K). The luminescence decay curves were recorded in the range of 0.04 to 10 ms, using a SPEX 1934D phosphorimeter coupled to the spectrofluorimeter.

2.2. Synthesis of coordination compounds

2.2.1. Synthesis of the $[Ln(acac)(NO_3)_2(phen)_2] \cdot H_2O$ complexes

The $[Ln(acac)(NO_3)_2(phen)_2]$ complexes (where Ln: Eu^{3+} and Gd^{3+}) were synthesized in the yield around 60%, following the methodology adapted from the literature [29]. In this case, the preparation of the $[Eu(acac)(NO_3)_2(phen)_2]$ complex has been presented as representatively. Firstly, the pH of a methanol solution containing 0.071 g (0.71 mmol) of acetylacetone (Hacac) was adjusted to approximately 7 by the addition of ammonium hydroxide (NH_4OH) ethanolic solution. After that, the resulting solution was added dropwise over a methanolic suspension of the precursor $[Eu(NO_3)_3(phen)_2]$ complex, 0.500 g (0.71 mmol), under stirring, resulting in a greenish-yellow solution

(Scheme 1). Again, the pH of the resulting solution was adjusted to ~7 and allowed to stand for slow solvent evaporation. After partial solvent evaporation, single crystals of the complex were obtained, which were collected, washed with methanol and then dried under reduced pressure. The synthesis of the [$Ln(acac)_3(phen)$] complexes (**Eu3** and **Gd3)** are presented in the Supporting Information.

[Eu(acac)$(NO_3)_2$(phen)$_2$]·H_2O (**Eu1**). Yield: 459.18 mg (60%). FT-IR (in KBr/cm_1): 3568 (w), 3049 (w), 1597 (s, C=O and C=C), 1517 (s), 1425 (s), 1392 (s), 1319 (m), 1263 (m), 848 (s), 729 (s), 427 (w). calcd: C, 46.23; H, 3.34; N, 11.15; Eu, 20,17 %, found: C, 46.21; H, 3.56; N, 11.16; Eu, 21.30%.

[Gd(acac)$(NO_3)_2$(phen)$_2$]·H_2O (**Gd1**). Yield: 302.72 mg (58%). FT-IR (in KBr/cm_1): 3566 (w), 3500 (w), 3064(w), 1600 (s, C=O and C=C), 1517 (s), 1425 (s), 1392 (s), 1319 (s), 1267 (m), 1217 (m), 1099 (m), 848 (s), 777 (m), 729 (s), 636 (w), 474 (w). calcd: C, 45.90; H, 3.32; N, 11.08; Gd, 20.17 %, found: C, 44.56; H, 3.01; N, 11.80; Eu, 20.79%.

2.2.2. Synthesis of the [$Ln(bza)(NO_3)_2(phen)_2]\cdot H_2O$ complexes

The synthesis of the [$Ln(bzac)(NO_3)_2(phen)_2$] complexes (where Ln: Eu^{3+} and Gd^{3+}) were performed in the yield at around 35% from the reactions between the β-diketone ligands and the lanthanide nitrates ethanol solutions. This procedure was adopted because the precursor complexes [$Ln(NO_3)_3(phen)_2$] were not quite soluble in the methanolic solution containing bzac ligand. The preparation of the [$Eu(bzac)(NO_3)_2(phen)_2$] complex has been presented as representatively.

To an ethanol solution (30 mL) containing bzac (1.00 g, 4.46 mmol) and phen (1.24 g, 4.46 mmol) under stirring, was added dropwise an ethanol solution (30 mL) of europium nitrate (0.56 g, 1.49 mmol). Three drops of concentrated nitric acid, HNO_3, was added to the solution and its pH was then adjusted to approximately pH 6 by using hydrated ethanol NaOH (0.01 $mol\cdot L^{-1}$) solution. The reaction mixture was allowed to stand overnight at room temperature, yielding a crystalline solid complex that was filtered, washed with ethanol, and dried under reduced pressure (Scheme 1). Although we obtained small amounts of crystalline sample, the single crystals were not suitable to record XRD data. The synthesis of the [$Ln(bza)_3(phen)$] complexes (**Eu4** and **Gd4)** are presented in the Supporting Information.

[Eu(bzac)(NO$_3$)$_2$(phen)$_2$]·H$_2$O (**Eu2**). Yield: 151 mg (35%). FT-IR (in KBr/cm_1): 3427 (w), 3066 (w), 2484 (w), 1595 (s, C=O and C=C), 1570 (s), 1517 (s), 1452 (s), 1421 (s), 1396 (s), 1315 (s), 1207 (m), 1143 (m), 1105 (m), 839 (m), 727(m), 636 (w), 563 (w), 522(w). calcd: C, 50,07; H, 3,34; N, 10,30; Eu, 18,63%, found: C, 50,60; H, 3,24; N, 10,42; Eu, 18,51 %.

[Gd(bzac)(NO$_3$)$_2$(phen)$_2$·H$_2$O] (**Gd2**). Yield: 293 mg (39%). FT-IR (in KBr/cm_1): 3365 (w), 3059 (w), 2914 (w), 1597 (s, C=O and C=C), 1558 (s), 1525 (s), 1456 (s), 1409 (s), 1396 (s), 1280 (m), 1068 (m), 950 (m), 842 (m), 763 (s), 709 (s), 559 (w). calcd: C, 49.75; H, 3.32; N, 10.24; Gd, 19.16%, found: C, 50.60; H, 3.24; N, 10.42; Gd, 18.92 %.

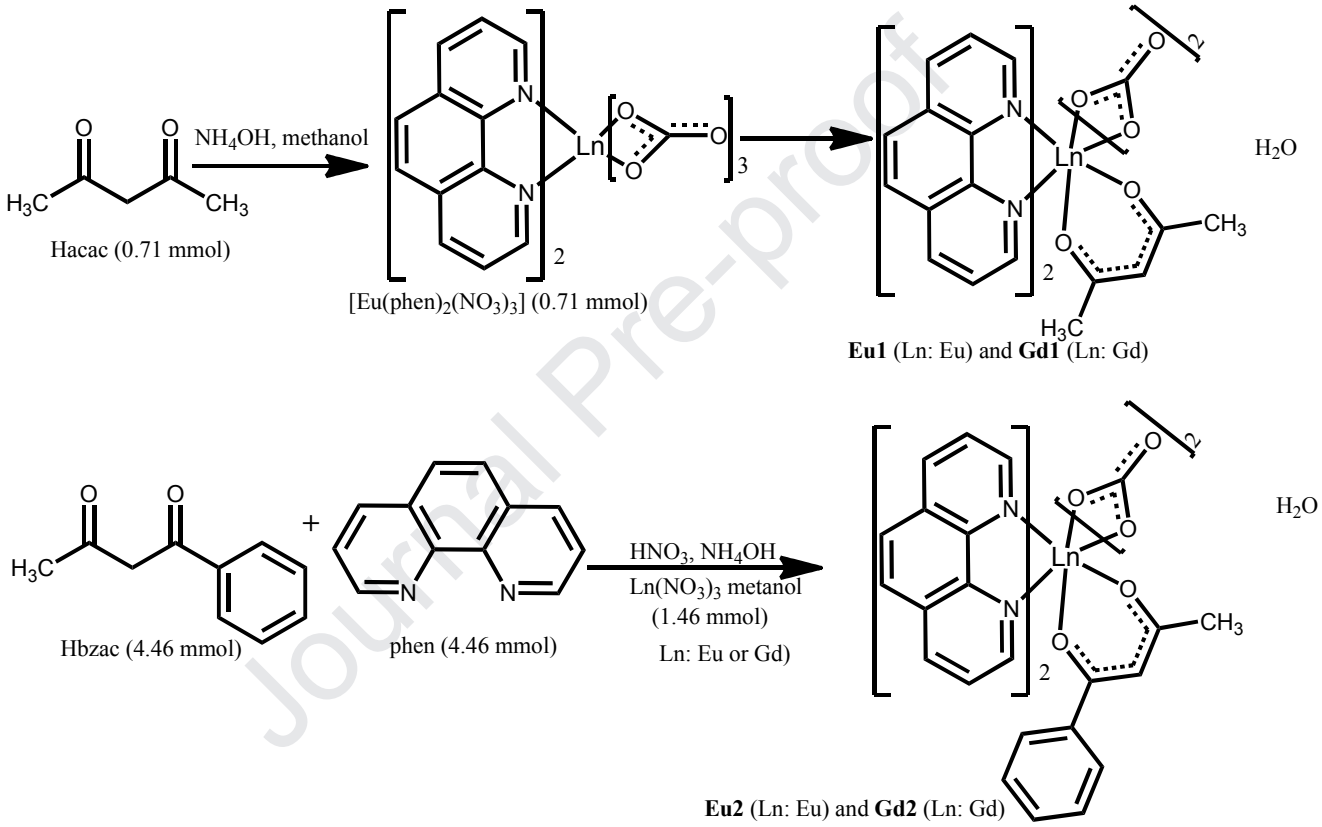

Scheme 1. Synthetic route for [Ln(β-dik)(NO$_3$)$_2$(phen)$_2$] complexes (Ln = Eu^{3+} and Gd^{3+}; β-dik = acac and bzac).

2.3. In silico experiments

The optimized geometries for all the europium complexes were obtained using the SPARKLE/PM3 [17] method implemented in the MOPAC2016 program [30]. Also, the frequency calculation of the optimized structures was done with the same method. The X-

ray crystal structure of the complex **Eu1** was used as starting point and it was also used to generate the input geometry for complex **Eu2**, where the methyl group in the β-diketonate molecule was substituted by a phenyl (phen) one. Scan calculations performing geometry transformations from **Eu1** and **Eu2** (coordination number equals 10) to [Eu(acac)$_3$(phen)] (**Eu3**) and [Eu(bzac)$_3$(phen)] (**Eu4**) (coordination number equals 8) were done using the same procedure. This scan consists of separation from a phen ligand concerning the Eu^{3+} ion. The purpose is to understand how the Eu^{3+} ion behaves in terms of Ω_λ with this geometry transformation (or the effect of a ligand leaving). To be more concise, in a certain step, two NO_3^- were substituted by two β-dik to guarantee that the last step has the same structure as the [Eu(β-dik)$_3$(phen)] one.

Density functional theory (DFT) calculations with the B3LYP functional [31–34] and aug-cc-pVDZ basis set [35] were carried out in the isolated ligands at the complexes structures. When employed a localization method (it was used the Pipek-Mezey one), the effective polarizabilities α' can be estimated by the sum over polarizabilities in regions nearby the coordinated atoms. This quantity (α') represents the chemical environment polarization capability close to the Ln^{3+} [18]. All this procedure was performed with the GAMESS program [36].

The theoretical intensity parameters were calculated with the JOYSpectra software [37], in which the quantities α' and g are input data while the α_{OP} is internally calculated using Eq. (S4). Further information is found in the Theoretical intensity parameters section in the Supporting Information.

3. Results and discussion

3.1. Structural analysis

Crystal collection parameters and structure refinement data for [Eu(acac)(NO$_3$)$_2$(phen)$_2$]·H$_2$O compound are presented in Table 1. The Crystallographic Information File (CIF) containing the complete information on the studied structure was deposited in the Cambridge Crystallographic Data Centre (CCDC) database under the number 1991792, where it can be obtained upon request at www.ccdc.cam.ac.uk/data_request/cif.

The hexagonal shape single crystals of the compound **Eu1** was obtained from the solvent evaporation technique. The compound crystallizes in a monoclinic spatial group P2/n and the value of Z = 2, presenting similar structural properties as the similar Tb^{3+}-complex reported in reference [29], in which the lattice water molecule forms a hydrogen bond between the NO_3^- groups of two complexes (Fig. 1a). Furthermore, there are π–π interactions between phen molecules with centroid····centroid, centroid····plane and horizontal displacement distances equal to 3.761, 3.411 and 1.58 Å, respectively. These structural results indicate that intermolecular stacking interactions are essential to solid-state stabilization (Fig. 1b).

The coordinating polyhedron may be described as a bi-capped distorted square antiprism (Figs. 1c and 1d), in which the Eu^{3+} ion has a coordination number (CN) equal to 10, coordinated by four oxygen atoms from two NO_3^- groups (O3', O2', O3 and O4), two oxygen atoms from the acetylacetonate ion (O4'and O4), and four nitrogen atoms from the two molecules of the 1,10-phenanthroline ligand (N1', N2', N1 and N2), are coordinated to the lanthanide ion (Fig. 1d). The angles (O–Eu–O and N–Eu–N) and bond distances (Eu–O and Eu–N) are shown in Table 2. As can be seen, the shorter Eu–O bond lengths involve oxygen atoms from the acac ligand, with Eu–O4 bond length equals 2.339 Å for both bonds.

Table 1. Crystal and structure refinement data for $[Eu(acac)(NO_3)_2(phen)_2]$ (complex **Eu1**).

Formula	$C_{29}H_{25}N_6O_9Eu$
F_w (g.mol^{-1})	753.50
Crystal system	Monoclinic
Space group	P2/n
a (Å)	11.1986
b (Å)	9.7154
c (Å)	13.3217
α (°)	90.0
β (°)	101.569
γ (°)	90.0
V (Å^3)	1419.94
Temperature (K)	293
Z	2
D_{calc} (g·cm^{-3})	1.762
Crystal size (mm)	0.11 × 0.36 × 0.48
μ(Mo Kα) (cm^{-1})	2.276
Measured reflexions/uniques	30667 / 3841
R_{int}	0.048
Observed reflexions [$F_o^2>2\sigma(F_o^2)$]	3632
Refined parameters	206
R_1	0.0232

wR_2	0.0487
GOF	1.068

This result indicates that the β-diketonate ligand is symmetrically coordinated with the metallic center. It is noteworthy that not only the coordination polyhedron but also the molecular symmetry is almost remained from the substitution of one nitrate ion in the precursor $[Eu(NO_3)_3(phen)_2]$ complex [29,38] by an acac molecule in the first coordination sphere of the Eu^{3+} ion (Fig. S1). The root mean square deviation (RMSD) between common parts of the precursor and **Eu1** complexes is 0.590 Å.

A comparison between the X-ray diffraction structures of the **Eu1** and $[Eu(acac)_3(phen)]$ compounds [10,13] reveals two considerable differences. Firstly, the Eu-O and Eu-N bond lengths are significantly shorter in the former compound. Second, the acac ligand is symmetrically coordinated to the europium ion, which presents both Eu–O bond distances equal to 2.339 Å compound **Eu1**. In contrast, the three acac ligands in the $[Eu(acac)_3(phen)]$ complex have different Eu–O bond distances around 2.362-2.409 Å. This structural behavior may be owing to the lower steric hindrance in the first coordination sphere of the lanthanide ion. It is noteworthy that both NO_3^- and phen ligands are asymmetrically coordinated to the Eu^{3+} ion in the compound **Eu1**, presenting bond distances of 2.533 and 2.682 Å ($Eu–O_{NO3}$) and 2.594 and 2.652 Å (Eu–N1 and Eu–N2), respectively.

1

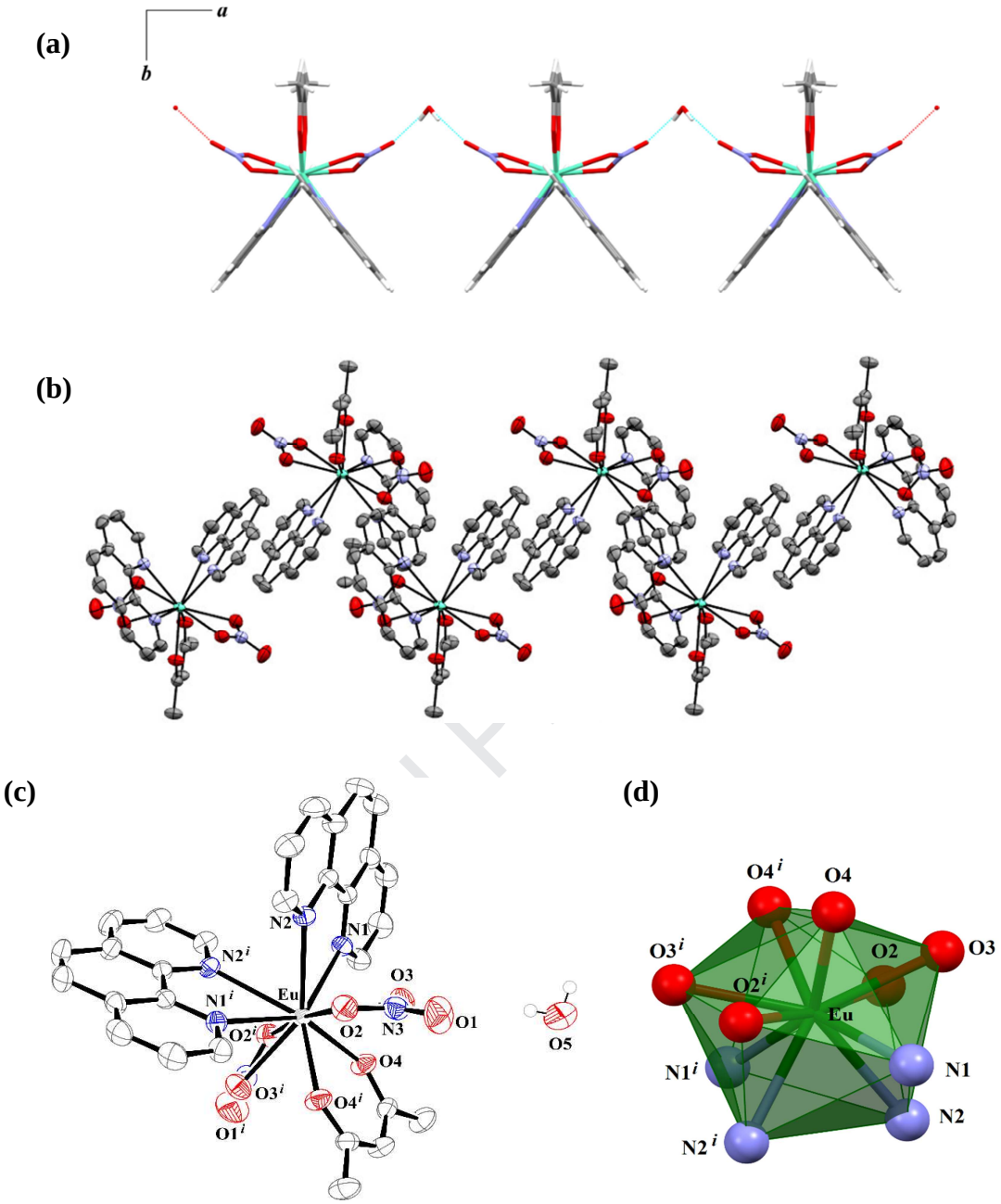

Fig. 1. (a) Projection of the structure in the crystallographic axis ***c*** showing the hydrogen bonding. (b) Part of the crystal structure showing π−π interactions between phen molecules. Symmetry code: 1.5 - *x*, *y*, ½ - *z*. (c) Ortep representation of $[Eu(acac)(NO_3)_2(phen)_2]$ (**Eu1**) complex and (d) Coordination polyhedron of the $[Eu(acac)(NO_3)_2(phen)_2]$ complex.

Table 2. Selected bond distances and angles for $[Eu(acac)(NO_3)_2(phen)_2]$ (complex **Eu1**).

Bond distances (Å)			
Eu–N1	2.594(2)	Eu–O3	2.533(2)
Eu–N2	2.652(2)	Eu–O4	2.339(2)
Eu–O2	2.682(2)		
Bond angles (°)			
N1–Eu–N2	62.46(5)	N2–Eu–N2^{i}	70.13(7)
N1–Eu–N2^{i}	80.60(5)	N2–Eu–N1^{i}	80.60(5)
N1–Eu–N1^{i}	135.07(7)	N2–Eu–O2	66.02(5)
N1–Eu–O2	111.03(5)	N2–Eu–O3	73.99(5)
N1–Eu–O3	75.11(5)	N2–Eu–O2^{i}	120.01(5)
N1–Eu–O2^{i}	71.64(5)	N2–Eu–O3^{i}	143.01(5)
N1–Eu–O3^{i}	120.08(5)	N2–Eu–O4	130.31(5)
N1–Eu–O4	146.20(5)	N2–Eu–O4^{i}	131.83(5)
N1–Eu–O4^{i}	77.44(5)	N1^{i}–Eu–O2	71.63(5)
N2^{i}–Eu–O2	120.01(5)	N1^{i}–Eu–O3	75.11(5)
N2^{i}–Eu–O3	143.01(5)	N1^{i}–Eu–O4	77.44(5)
N2^{i}–Eu–O4	131.83(5)	O2–Eu–O3	48.51(5)
O2–Eu–O4	64.89(5)	O4–Eu–O4^{i}	73.24(7)
O2–Eu–O4^{i}	109.42(5)	O2–Eu–O2^{i}	173.44(7)
O3–Eu–O4	79.55(5)	O3–Eu–O3^{i}	142.74(8)
O3–Eu–O4^{i}	70.4(5)	O2–Eu–O3^{i}	128.75(5)

3.2. Fourier transform infrared spectroscopy

FTIR absorption spectra of the compounds **Eu1** and **Eu2** recorded in the range of 4000 to 400 cm^{-1} are shown in Fig. S2. All spectra exhibit a broad band within 3500–2700 cm^{-1} that is attributed to the stretching vibrational ν(O–H) modes of the uncoordinated water molecule. The intense bands around 1597 cm^{-1} is ascribed to the carbonyl vibrational ν(C=O, C=C) modes of the β–diketonate ligands. These absorption bands are shifted to lower wavenumbers as compared to the uncoordinated ligands, suggesting that β–diketonate ligands are coordinated to the Ln^{3+} ion in chelating mode. The characteristic absorption bands assigned to the stretching vibrational ν(C=C) mode of the coordinated phen ligands are shift to higher wavenumber (1590 cm^{-1}) as compared with that one for uncoordinated this ligand (1561 cm^{-1}) [39]. In addition, FTIR spectra also exhibit two characteristic bands around 1820 and 1767 cm^{-1} due to the $\nu_1 + \nu_4$ combination modes, reflecting the bidentate chelating coordination mode of the nitrate groups.

3.3. Thermal decomposition analysis

The TGA curves of the compounds **Eu1 and Eu2** present a weight-loss event in the temperature interval from 70 to 150°C (Fig. S4) attributed to the dehydration process due to the release of lattice water molecules. On the other hand, above 200 °C, two consecutive weight loss events are corresponding to the thermal decomposition of the organic ligand moieties. The final residue may be assigned to the corresponding lanthanide oxides (Eu_2O_3).

3.4. Photophysical properties

Diffuse reflectance spectra of [Ln(β–dik)$(NO_3)_2$(phen)$_2$] complexes (Ln: Gd or Eu) show strong absorption bands in the range of 200 to 450 nm ascribed to the $S_0 \rightarrow S_n$ ($\pi\pi^*$ or mixed $n\pi^*$) transitions from the diketonate and 1,10–phenantroline ligands (Fig. 2). Similar absorption bands are also observed in the reflectance spectra of well–known [Ln(β–dik)$_3$(phen)] complexes (Fig. 3). These spectra for compounds **Eu1** and **Eu2** (Fig. 2) exhibit shoulders bands in the longer wavelength regions, as compared with similar Gd^{3+} systems. This spectral behavior may be attributed to the presence of lower–energy LMCT transitions in the Eu^{3+}–complexes with acac and bzac ligands.

The spectra of the Eu^{3+}–compounds were deconvoluted to investigate the behavior of LMCT transition in these kinds of complexes. The the best fit by a sum of Gaussian bands are shown in Fig. 4. Interestingly, the results show that the lowest–energy components due to the LMCT bands are redshift for both **Eu1** (23529 cm^{-1}, 425 nm) and **Eu2** (22421 cm^{-1}, 446 nm) complexes, as compared with **Eu3** (28248 cm^{-1}, 454 nm) and **Eu4** (26809 cm^{-1}, 373 nm) complexes (Fig. 2 and 3). These data strongly indicate that structural features play important roles on the charge transfer from diketonate ligands to the Eu^{3+} ion in the complexes **Eu1** and **Eu2**, due to the shorter Eu–O bond distances in these complexes, as compared with Eu–O bond distances in the [Ln(β–dik)$_3$(phen)] [10].

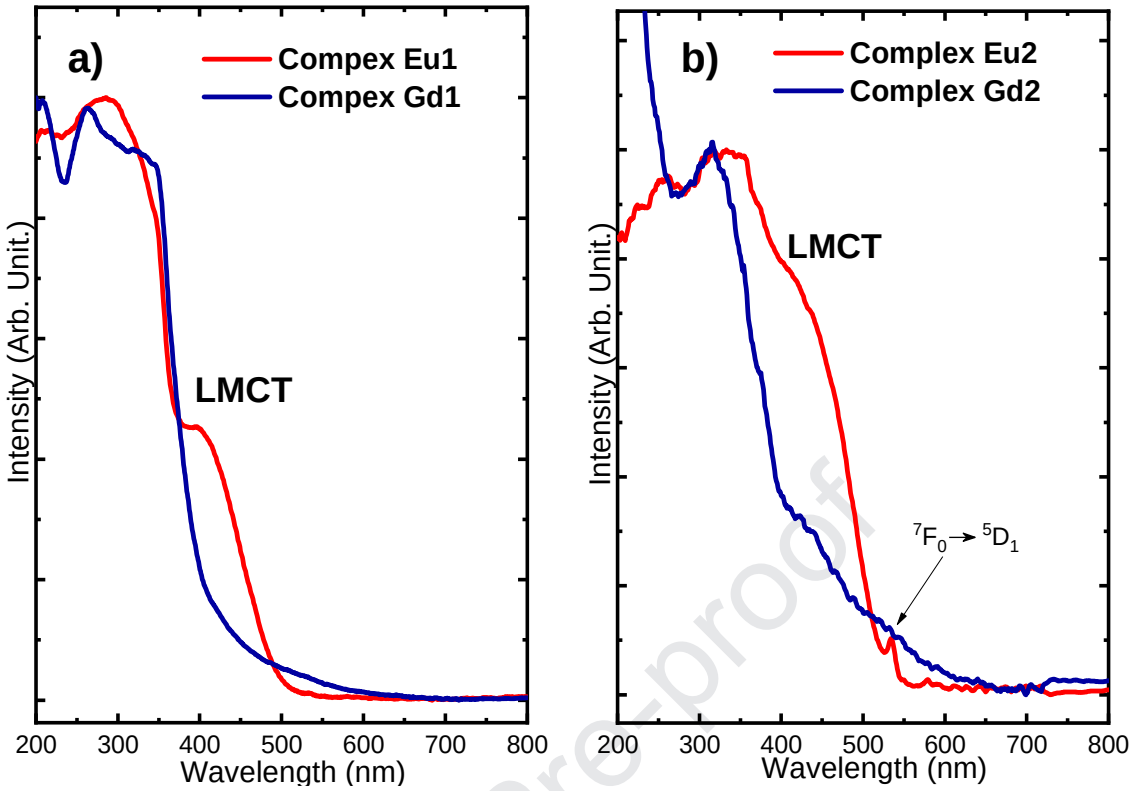

Fig. 2. Diffuse reflectance spectra of the (a) [Ln(acac)$(NO_3)_2$(phen)$_2$] (**Eu1** and **Gd1)** and (b) [Ln(bzac)$(NO_3)_2$(phen)$_2$] **(Eu2** and **Gd2)** complexes (Ln: Eu and Gd), recorded in the solid state.

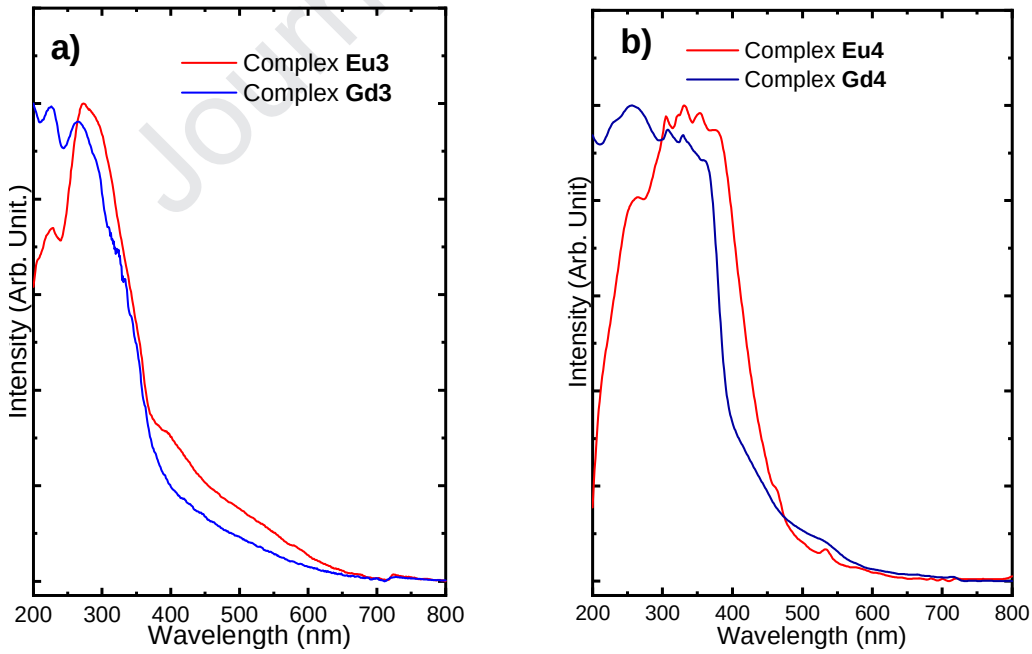

Fig. 3. Diffuse reflectance spectra of the (a) [Ln(acac)$_3$(phen)](**Eu3** and **Gd3**) and (b) [Ln(bzac)$_3$(phen)] (**Eu4** and **Gd4**) complexes (Ln: Eu and Gd), recorded in the solid state.

The excitation spectra of the [Eu(β-dik)$(NO_3)_2$(phen)$_2$] recorded at 77 K present broad bands in the higher energy region attributed to the $S_0 \rightarrow S_1$ transition, indicating the luminescence sensitization of the Eu^{3+} ion by β-diketonate ligands (Figs. 5a and 5b). However, it is very important to note the rapid decrease of the excitation curve around 380 and 360 nm for complexes **Eu1** and **Eu2**, respectively**,** coinciding with the spectral region of the LMCT absorption as observed in the diffuse reflectance spectra (Fig. 4). This spectral behavior indicates the presence of efficient energy deactivating channels close to excited states of the diketonate ligands. According to the spectral data, these deactivation channels may be assigned to the charge transfer states among diketonate–to–Eu^{3+} ion. Moreover, the excitation spectra display narrow absorption bands attributed to the 4f–4f transitions (Figs. 5a and 5b).

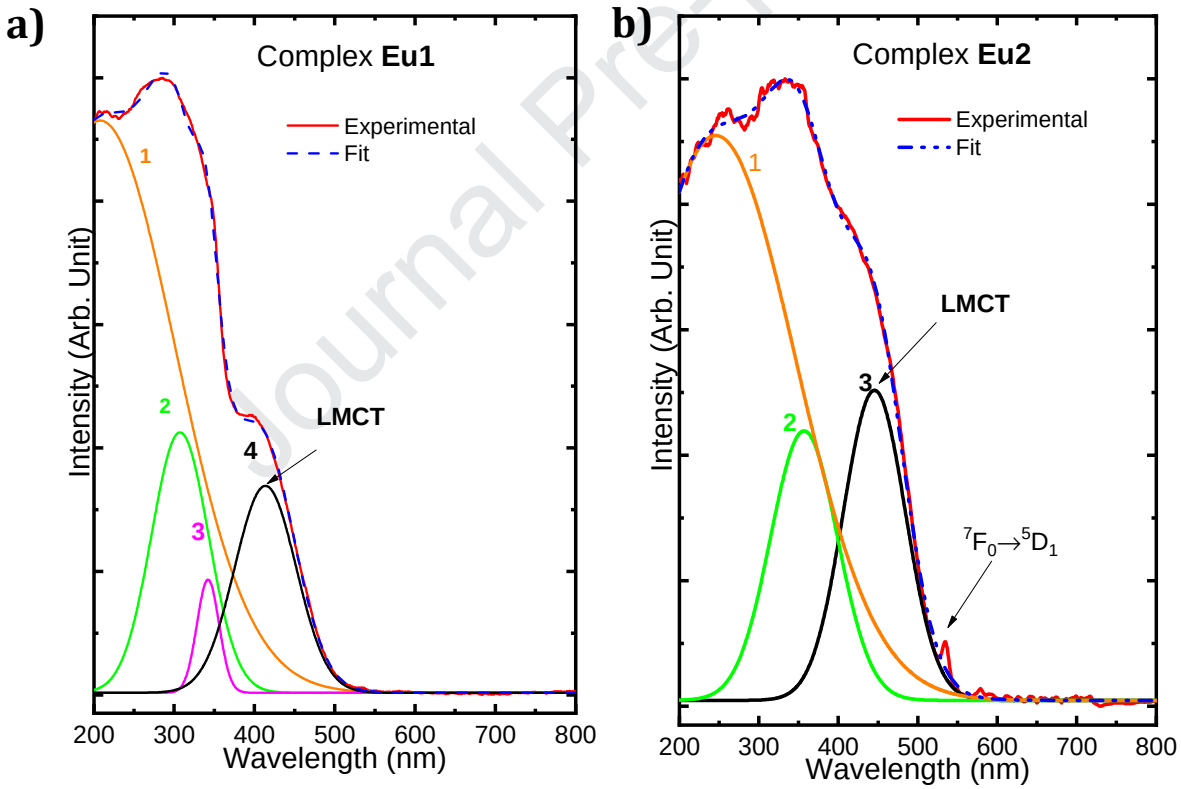

Fig. 4. Deconvoluted diffuse reflectance spectra of the (a) [Eu(acac)$(NO_3)_2$(phen)$_2$] (**Eu1**) and (b) [Eu(bzac)$(NO_3)_2$(phen)$_2$] **(Eu2)** complexes, recorded in the solid-state. Experimental spectra are shown in red solid lines, total Gaussian fit (as dashed lines) and individual Gaussian bands are also shown.

The excitation band assigned to the $^7F_0 \rightarrow {}^5D_2$ transition of the Eu^{3+} complexes exhibits very weak relative absorption intensity for the complex **Eu1**. It is noteworthy that this band show higher relative intensities for the complex **Eu2**, indicating that $^5D_0$ emitting level of the Eu^{3+} ion is more efficiently populated via direct excitation process.

The emission spectra of complexes **Eu1** and **Eu2** recorded in the range of 500–730 nm at liquid nitrogen temperature under excitation at 350 nm from the β-diketonate ligands are shown in Figs 5c and 5d. These spectra are characterized by narrow emission bands, emanating from the $^5D_0$ emitting level to the ^7F_J levels (J = 0, 1, 2, 3, and 4) of the Eu^{3+} ion.

1

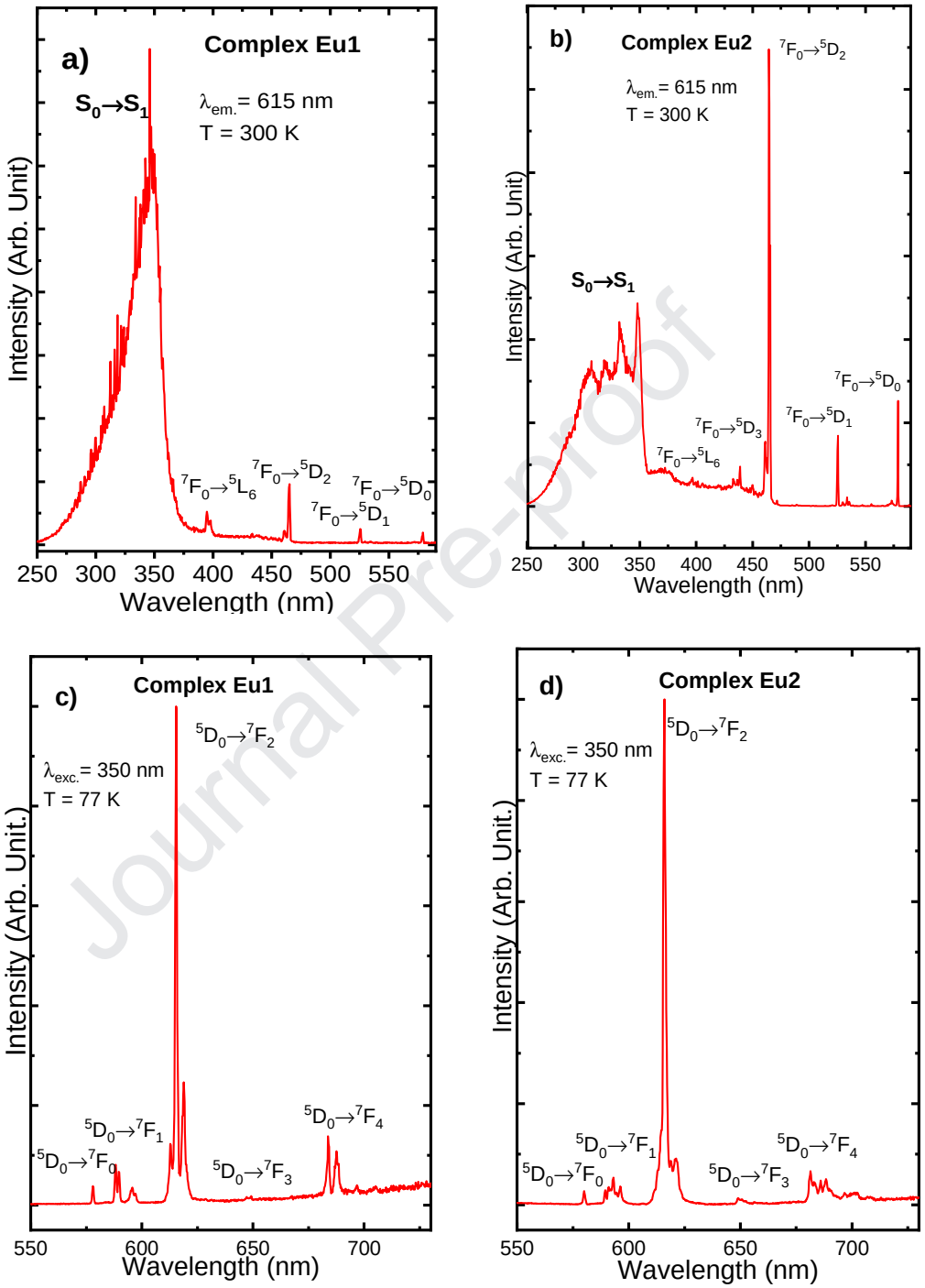

Fig. 5. Excitation spectra of (a) $[Eu(acac)(NO_3)_2(phen)_2]$ (**Eu1**) and (b) $[Eu(bzac)(NO_3)_2(phen)_2]$ (**Eu2**) complexes in the solid-state recorded at liquid nitrogen temperature with emission monitored on the $^5D_0 \rightarrow ^7F_2$ transition around 616 nm. Emission spectra of the (c) $[Eu(acac)(NO_3)_2(phen)_2]$ (**Eu1**) and (d) $[Eu(bzac)(NO_3)_2(phen)_2]$ (**Eu2**) complexes recorded at liquid nitrogen temperature with excitation monitored on the $S_0 \rightarrow S_1$ diketonate ligand transition around 350 nm.

The experimental values of the spontaneous-emission coefficients ($A_{0\rightarrow J}$) ascribed to the $^5D_0 \rightarrow {}^7F_J$ (where, J = 0, 2, 3 and 4) transitions of the Eu^{3+} ion have been determined from the spectral data by [21,22]:

$$A_{0\rightarrow J} = \left(\frac{S_{0\rightarrow J}}{S_{0\rightarrow 1}}\right) A_{0\rightarrow 1} \quad (1)$$

where $S_{0\rightarrow J}$ and $S_{0\rightarrow 1}$ are the areas under the emission bands assigned to the $^5D_0 \rightarrow {}^7F_J$ and $^5D_0 \rightarrow {}^7F_1$, respectively. In this equation $A_{0\rightarrow 1} \cong 50\ s^{-1}$ for index of refraction $n = 1.5$ [40]. Furthermore, making the sum of these values ($\sum A_{0\rightarrow J} = A_{rad}$) and using the lifetimes (τ) of the emitting level ($^5D_0$), it is possible to calculate the non-radiative component A_{nrad} by using the following relationship:

$$A_{nrad} = A_{total} - A_{rad} = \tau^{-1} - A_{rad} \quad (2)$$

The intrinsic quantum yield Q_{Ln}^{Ln} [40,41], is the quotient between the A_{rad} component and the total one A_{total}.

$$Q_{Ln}^{Ln} = \frac{A_{rad}}{A_{total}} = A_{rad}\tau \quad (3)$$

Exclusively for the case of Eu-based compounds, the experimental intensity parameters (Ω_λ, λ = 2 and 4) can be determined as follows [40,41]:

$$\Omega_\lambda = \frac{3\hbar c^3 A_{0\rightarrow\lambda}}{4e^2\omega^3\chi\langle {}^7F_\lambda \| U^{(\lambda)} \| {}^5D_0\rangle^2} \quad (4)$$

where $\langle {}^7F_\lambda \| U^{(\lambda)} \| {}^5D_0\rangle^2$ are the square reduced matrix elements with values 0.0032 and 0.0023 for $\lambda = 2$ and 4, respectively [42]. $\chi = n(n^2+2)^2/9$ is the Lorentz local field correction. It is possible to observe that the Ω_2 parameter values for complexes **Eu1** and **Eu2** are close to the values of Ω_4. (Table 3). However, the Ω_4 parameter values for tris–β-diketonate complexes **Eu3** and **Eu4** are at around twice as low.

Fig. S7 shows the luminescence decay curves of complexes **Eu1** and **Eu2** recorded at 77K under excitation and emission monitored at 350 and 616 nm, respectively. The lifetime (τ) values of the $^5D_0$ emitting level were determined by fitting these curves to a single exponential function, indicating the presence of only one emissive Eu^{3+} center in each complex. Despite experimental evidence of the LMCT states, the τ values for complexes **Eu1** and **Eu2** are close to those obtained for Eu^{3+}-tris-diketonate complexes (Table 3), suggesting that

the luminescence quenching process in those complexes take place via deactivation of the ligand excited states, instead of a direct deactivation of the $^5D_0$ emitting level.

Therefore, the A_{rad} values for complexes **Eu1** and **Eu2** are quite similar to those for tris–diketonate complexes. Interestingly, the values of intrinsic emission quantum yield (Q_{Eu}^{Eu}) also show similar behavior, which is also consistent with the fact of LMCT states are acting more efficiently as a luminescence quencher by deactivating the excited states of the ligands than via direct deactivation of Eu^{3+} emitting level. This explanation is consistent with excitation spectral data (Fig. 5a and 5b) and with A_{nrad} values.

Table 3. Luminescence lifetimes τ (in ms), intensity parameters Ω_λ (in 10^{-20} cm^2), radiative A_{rad} (in s^{-1}), non–radiative A_{nrad} (in s^{-1}) and total A_{total} (in s^{-1}) emission rates and intrinsic quantum yield Q_{Eu}^{Eu} (in %) of the compounds with the general formula [Eu(β–dik)$(NO_3)_2$(phen)$_2$] and [Eu (β–dik)$_3$(phen)]. All the data below were obtained at 77 K.

Label	Compound	τ	Ω_2	Ω_4	A_{rad}	A_{nrad}	A_{total}	Q_{Eu}^{Eu}
Eu1	[Eu(acac)$(NO_3)_2$(phen)$_2$]	0.666	11.1	9.6	573	928	1501	38
Eu2	[Eu(bzac)$(NO_3)_2$(phen)$_2$]	0.729	14.8	10.1	670	701	1371	48
Eu3	[Eu(acac)$_3$(phen)]	0.678	14.6	5.2	600	874	1474	41
Eu4	[Eu(bzac)$_3$(phen)]	0.501	20.3	4.3	754	1242	1996	38

3.5. Theoretical intensity parameters

The intensity parameters (Ω_λ) of the Eu^{3+} ion in the complexes were also theoretically investigated, considering both forced electric dipole (FED) and the polarizability dependent dynamic coupling (DC) mechanisms [18,19,43–52]. This theoretical investigation was performed by using the Simple Overlap Model (SOM) for the FED [19,48] and the Bond Overlap Model (BOM) [18] for the DC mechanism. In this line, the charge factors (g_j) and polarizabilities (α_j) can be determined in order to evaluate the role of the chemical environment on the intensity parameters. It is important to mention that α is partitioned into α_{OP} and α' (Eq. S3) that are associated to the polarizabilities of the chemical bonds and of the ligand regions that can direct or indirectly affect the chemical environment of the Ln^{3+} ion, respectively.

The optimized molecular structure of the complex **Eu1** is in excellent agreement with X-ray structure with RMSD errors equal to 0.3978 and 0.2261 Å, for all atoms in the

complex molecule and when considered only the coordination polyhedron, respectively. This finding indicates that the theoretical method used (Sparkle/PM3) yields a good description of the molecular geometries of the lanthanide complexes (Fig. S9). In addition, the frequencies calculations indicated that all the studied compounds are at a local minimum, not containing imaginary frequencies.

In the present work, the values of charge factors (g) were assumed to be ca. 1.0, which is the mean value for all studied types of ligands and is reasonably close to the ones that are usually obtained for this kind of ligand. Additionally, g values compose the FED mechanism (Eq. S2), being responsible by 0.1 – 3.0% of the Ω_λ values for Eu^{3+}–β–diketonate complexes [18]. On the other hand, α' were determined using localized orbitals in optimized molecular structures of the complexes. The α' values were assigned into account two ligand molecular regions (Fig. 6): *i*) The lone pair (LP) region located on the coordinating atoms (used for neutral ancillary ligands) and *ii*) The region 1, which includes the LP region and the LMOs located at the spatial region defined by one chemical bond away from the Eu^{3+} ion (used for negative charged main ligands). Table 4 summarizes the calculated $\bar{\alpha}_{mol}$ α', α_{OP} and g values for the β–diketonate, phen and NO_3^- ligands.

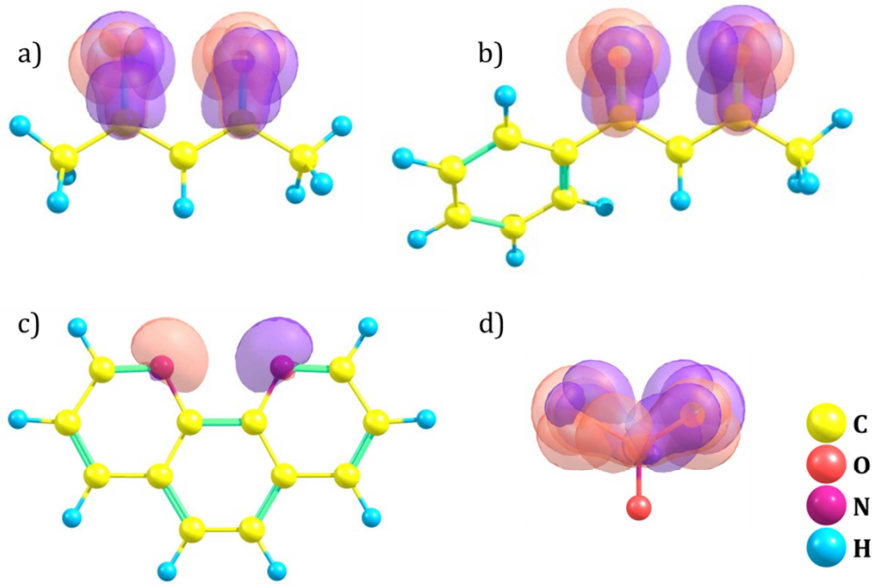

Fig. 6: LMO superpositions nearby the ligating atoms for a) acac, b) bzac, c) phen and d) NO_3^- ligands, obtained with an isosurface of 0.1 e/a_0^3. In the case of phen it was considered only the polarizability of the lone-pair orbitals, since phen has weaker bonding, in contrast to the charged ligands.

Table 4. Ligand and Eu–L bonds properties for different ligands. Mean molecular isotropic polarizability $\bar{\alpha}_{mol}$ (in Å^3), effective ligand polarizability α' (in Å^3), Eu–L chemical bonds overlap polarizability α_{OP} (in 10^{-2} Å^3) and charge factor g (dimensionless).

Compound	Ligand	$\bar{\alpha}_{mol}$		α_{OP}	α'	g
Eu1	acac	14.78	O(1)	3.31	2.6	1.0
			O(2)	3.31	2.6	1.0
	NO_3^-	4.48	O(3)	2.84	1.5	1.0
			O(4)	2.84	1.5	1.0
			O(5)	2.84	1.5	1.0
			O(6)	2.84	1.5	1.0
	Phen	24.74	N(7)	2.51	0.45	1.0
			N(8)	2.44	0.45	1.0
			N(9)	2.51	0.45	1.0
			N(10)	2.44	0.45	1.0
Eu2	bzac	23.49	O(1)	3.30	2.5	1.0
			O(2)	3.30	2.5	1.0
	NO_3^-	4.48	O(3)	2.84	1.5	1.0
			O(4)	2.84	1.5	1.0
			O(5)	2.84	1.5	1.0
			O(6)	2.84	1.5	1.0
	Phen	24.74	N(7)	2.51	0.45	1.0
			N(8)	2.44	0.45	1.0
			N(9)	2.51	0.45	1.0
			N(10)	2.44	0.45	1.0
Eu3	acac	14.78	O(1)	3.37	2.6	1.0
			O(2)	3.36	2.6	1.0
			O(3)	3.38	2.6	1.0
			O(4)	3.38	2.6	1.0
			O(5)	3.36	2.6	1.0
			O(6)	3.37	2.6	1.0
	Phen	24.74	N(7)	2.55	0.45	1.0
			N(8)	2.56	0.45	1.0
Eu4	bzac	23.49	O(1)	3.37	2.5	1.0
			O(2)	3.38	2.5	1.0
			O(3)	3.38	2.5	1.0
			O(4)	3.39	2.5	1.0
			O(5)	3.37	2.5	1.0
			O(6)	3.38	2.5	1.0
	Phen	24.74	N(7)	2.56	0.45	1.0
			N(8)	2.56	0.45	1.0

It is noteworthy that the α', α_{OP} and g values for these ligands are close to those usually obtained for this class of ligands in different coordination compounds [18]. It can be observed that ligands phen and bzac that contain aromatic groups exhibit higher

molecular isotropic polarizabilities ($\bar{\alpha}_{mol}$) then the acac ligand. However, the higher values of α' and α_{OP} are obtained for acac, bzac and NO_3^- groups. Given that the molecular regions close to the oxygen donor atoms effectively play the most crucial role on the chemical environment, the α' values are more appropriate than $\bar{\alpha}_{mol}$ to describe the spectroscopic properties of the Eu^{3+} ion. Indeed, phen ligands are neutral, exhibiting smaller values of α' than negative charged ligands like acac, bzac and NO_3^-.

The [Eu(β–dik)$(NO_3)_2$(phen)$_2$] (**Eu1** and **Eu2**) and [Eu(β–dik)$_3$(phen)] (**Eu3** and **Eu4**) compounds exhibit coordination numbers equals 10 and 8, respectively. Two factors can be highlighted as contributing to the observed variation of the Ω_λ experimental values for these compounds: 1) The change in the coordination number, which causes modifications in the coordination polyhedron geometry; and 2) The exchange of ligands from two NO_3^- to two β–dik, which causes chemical environment modifications. Aiming to simulate these factors, theoretical calculations were done in order to observe the variations on the theoretical values of Ω_2, Ω_4 and its ratio (Ω_2/Ω_4). A geometry transformation was simulated from [Eu(β–dik)$(NO_3)_2$(phen)$_2$] to [Eu(β–dik)$_3$(phen)] complexes in several steps, as illustrated in Fig. 7.

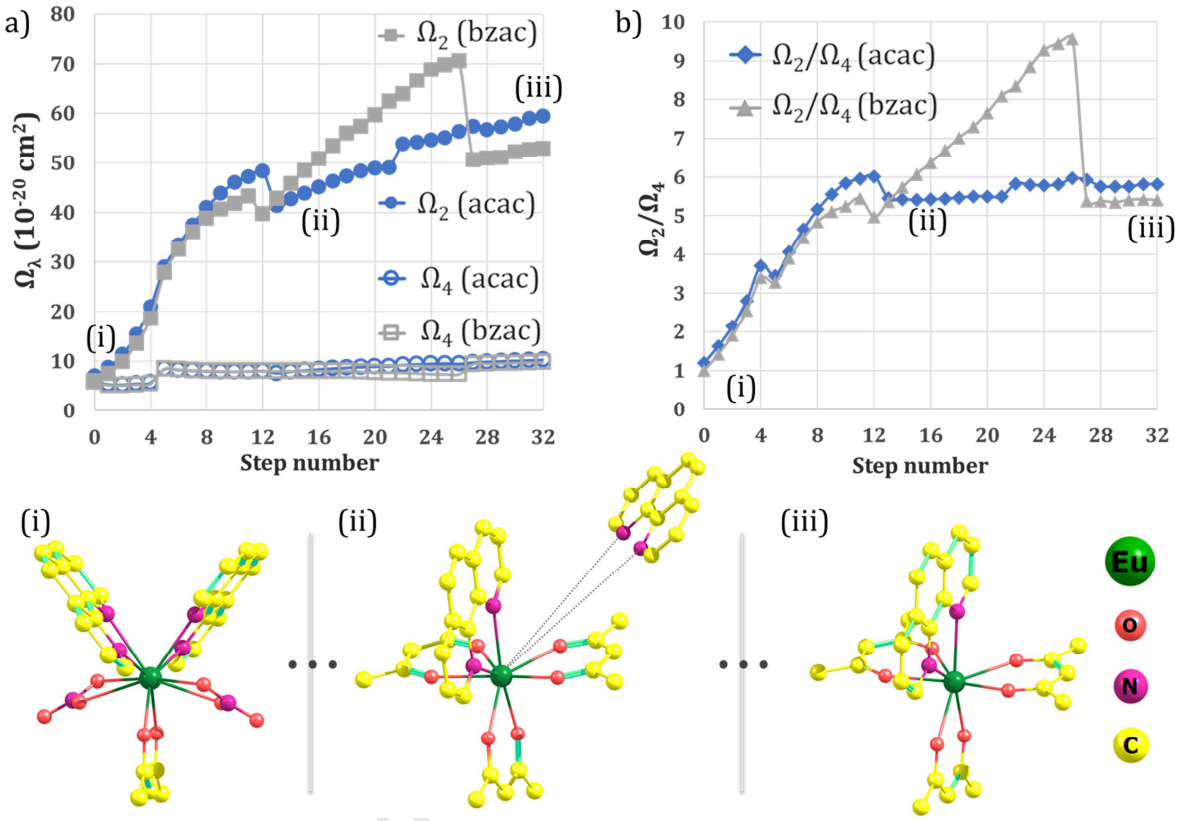

Fig. 7. Theoretical intensity parameters Ω_2 and Ω_4 (a) and their ratios Ω_2/Ω_4 (b) for acac and bzac in each complex following the simulated geometry transformation. Three geometries (i, ii, iii) are highlighted to indicate important geometry variations during the transformation

Starting with the Sparkle/PM3 optimized structure of the [Eu(β–dik)$(NO_3)_2$(phen)$_2$] complexes, successive steps were carried out in which, for each one, displacements of 0.2 Å were performed between one of the phen ligands and the Eu^{3+} ion, with the inicial Eu^{3+}–phen distance of 2.17 Å. For each one of these displacements, a new geometry optimization was done, with each new structure being used on the next step. At step 5, the two nitrate ligands were replaced by β–dik ligands. The increment in Eu^{3+}–phen distance was stopped at step 32, in which considerable structural changes were not observed. The final Eu^{3+}–phen distance was 8.57 Å for both acac and bzac complexes.

The theoretical intensity parameters calculations with JOYSpectra software were performed for the optimized structures in each step, from 1 to 32. For this, the α' values in

Table 4 were used for steps between 1 and 32. To simulate the chemical environment transformation in each intermediate step (2⋯31), the values of $\alpha'(NO_3^-) = 1.5$ Å (step 1, complexes **Eu1** and **Eu2**) were increased until they reach the $\alpha'(\beta-\text{dik})$ (acac or bzac) value, corresponding to the complexes **Eu3** and **Eu4**. The used values can be found in Table S1.

Fig. 7a and 7b summarize the Ω_2, Ω_4, and its ratio (Ω_2/Ω_4) variations for each studied transformation. It can be observed that, for acac and bzac compounds, from step 4 to 5, a sudden increase occurs in Ω_2 and Ω_4, being more pronounced in Ω_4, causing a decrease in Ω_2/Ω_4. This is a direct consequence of the modification from two NO_3^- to two β–dik imposed in the simulation. From step 12 (11) to 13 (12) for acac (or bzac), it is observed a big variation in the dihedral angle (in the coordination polyhedron) between the two new β–dik ligands. The calculated angle variation was from 88.8 to 3.6° for acac and from 70.1 to 41.6° for bzac. From steps 21 to 22 for acac (from 26 to 27 for bzac), it is observed other variation in the same dihedral angle from 18.3 to 4.5° for acac and from 65.6 to 24.6° for bzac.

The calculated variations indicate that the geometric alterations resulting from the removal of one phen ligand are, indeed, causing the experimentally observed variations in the Ω_2 and Ω_4 values. It is important to emphasize that the experimental ratios Ω_2/Ω_4 are: 1.15 for **Eu1**; 2.8 for **Eu3**; 1.5 for **Eu2** and 4.7 for **Eu2**. From Fig. 7b is possible to see that these values are ca. 1.0 for the mono β–dik species and ca. 5.0 – 5.5 for tris β–dik species. Given that the computational approach applied in this work does not perform any parameter fitting, it is possible to indicate a good agreement between experimental and theoretical results.

In general, it is possible to explain the increase of Ω_λ parameters from **Eu1** to **Eu2** by the slight increase in α' and geometric variation as a consequence of the aromatic ring in bzac ligand. Besides, the mono to tris β–dik variations present an increase of Ω_2 and a decrease of Ω_4 parameter, which may be explained by the geometry modifications as a consequence of the coordination number decrease and the ligand exchanges.

4. Conclusion

The theoretical and experimental structural data of the $[Eu(acac)(NO_3)_2(phen)_2]$(**Eu1**) and $[Eu(bzac)(NO_3)_2(phen)_2]$(**Eu2**) complexes reveals that

the diketonate ligands are symmetrically coordinated to the lanthanide ions. The luminescence properties of the Eu^{3+}–compounds are strictly dependent on the position of the ligand–to–metal charge transfer states (LMCT). These prepared complexes present an efficient depopulation of the excited ligand states by the LMCT states. Furthermore, the theoretical study reveals the role of α' and geometric variation on the increase of $\Omega_{2,4}$ of the complexes **Eu1** and **Eu2** to tris β–dik complexes **Eu3** and **Eu4**.

Declaration of Competing Interest

The authors declare that they have no known competing for financial interests or personal relationships that could have appeared to influence the work reported in this paper.

Acknowledgements

The authors are grateful for the financial support from the Conselho Nacional de Desenvolvimento Científico e Tecnológico (CNPq), the Coordenação de Aperfeiçoamento de Pessoal de Nível Superior (CAPES), the Fundação de Amparo à Pesquisa do Estado de São Paulo (FAPESP) and the Financiadora de Inovação e Pesquisa (FINEP). This work was developed within the scope of the project CICECO-Aveiro Institute of Materials, UIDB/50011/2020 & UIDP/50011/2020, financed by Portuguese funds through the FCT/MEC and when appropriate co-financed by FEDER under the PT2020 Partnership Agreement. ANCN thanks SusPhotoSolutions project, CENTRO-01-0145-FEDER-000005, Portugal for his grant.

Appendix A. Supporting information

References

[1] K. Singh, R. Boddula, S. Vaidyanathan, Versatile Luminescent Europium(III)−β-Diketonate-imidazo-bipyridyl Complexes Intended for White LEDs: A Detailed Photophysical and Theoretical Study, Inorg. Chem. 56 (2017) 9376–9390. doi:10.1021/acs.inorgchem.7b01565.

[2] P. Martin-Ramos, M. Ramos-Silva, Lanthanide-Based Multifunctional Materials: From OLEDs to SIMs, 1st ed., Elsevier, Amsterdam, 2018.

[3] D. Mara, F. Artizzu, B. Laforce, L. Vincze, K. Van Hecke, R. Van Deun, A.M. Kaczmarek, Novel tetrakis lanthanide β-diketonate complexes: Structural study, luminescence properties and

temperature sensing, J. Lumin. 213 (2019) 343–355. doi:10.1016/j.jlumin.2019.05.035.

[4] K. Gupta, A.K. Patra, A Luminescent pH-Responsive Ternary Europium(III) Complex of β-Diketonates and Terpyridine Derivatives as Sensitizing Antennae - Photophysical Aspects, Anion Sensing, and Biological Interactions, Eur. J. Inorg. Chem. 2018 (2018) 1882–1890. doi:10.1002/ejic.201701495.

[5] J. Wu, Y. Xing, H. Wang, H. Liu, M. Yang, J. Yuan, Design of a β-diketonate–Eu^{3+} complex-based time-gated luminescence probe for visualizing mitochondrial singlet oxygen, New J. Chem. 41 (2017) 15187–15194. doi:10.1039/C7NJ03696E.

[6] G.F. de Sá, O.L. Malta, C. de Mello Donegá, A.M. Simas, R.L. Longo, P.A. Santa-Cruz, E.F. da Silva, Spectroscopic properties and design of highly luminescent lanthanide coordination complexes, Coord. Chem. Rev. 196 (2000) 165–195. doi:10.1016/S0010-8545(99)00054-5.

[7] W.M. Faustino, O.L. Malta, G.F. de Sá, Intramolecular energy transfer through charge transfer state in lanthanide compounds: A theoretical approach, J. Chem. Phys. 122 (2005) 054109. doi:10.1063/1.1830452.

[8] W.M. Faustino, G.B. Rocha, F.R. Gonçalves e Silva, O.L. Malta, G.F. de Sá, A.M. Simas, Design of ligands to obtain lanthanide ion complexes displaying high quantum efficiencies of luminescence using the sparkle model, J. Mol. Struct. THEOCHEM. 527 (2000) 245–251. doi:10.1016/S0166-1280(00)00497-8.

[9] E.E.S. Teotonio, H.F. Brito, H. Viertler, W.M. Faustino, O.L. Malta, G.F. de Sá, M.C.F.C. Felinto, R.H.A. Santos, M. Cremona, Synthesis and luminescent properties of Eu^{3+}-complexes with 2-acyl-1 , 3-indandionates (ACIND) and TPPO ligands: The first X-ray structure of Eu–ACIND complex, Polyhedron. 25 (2006) 3488–3494. doi:10.1016/j.poly.2006.06.035.

[10] W.H. Watson, R.J. Williams, N.R. Stemple, The crystal structure of tris(acetylacetonato)(1,10-phenanthroline) europium(III), J. Inorg. Nucl. Chem. 34 (1972) 501–508. doi:10.1016/0022-1902(72)80428-7.

[11] D.R. van Staveren, G.A. van Albada, J.G. Haasnoot, H. Kooijman, A. Maria Manotti Lanfredi, P.J. Nieuwenhuizen, A.L. Spek, F. Ugozzoli, T. Weyhermüller, J. Reedijk, Increase in coordination number of lanthanide complexes with 2,2′-bipyridine and 1,10-phenanthroline by using β-diketonates with electron-withdrawing groups, Inorganica Chim. Acta. 315 (2001) 163–171. doi:10.1016/S0020-1693(01)00334-6.

[12] P.K. Shahi, A.K. Singh, S.K. Singh, S.B. Rai, B. Ullrich, Revelation of the Technological Versatility of the Eu(TTA) 3 Phen Complex by Demonstrating Energy Harvesting, Ultraviolet Light Detection, Temperature Sensing, and Laser Applications, ACS Appl. Mater. Interfaces. 7 (2015) 18231–18239. doi:10.1021/acsami.5b06350.

[13] Y. Fukuda, A. Nakao, K. Hayashi, Syntheses and specific structures of higher-order mixed chelate lanthanide complexes containing terpyridine, acetylacetonate, and nitrate ligands, J. Chem. Soc. Dalt. Trans. (2002) 527–533. doi:10.1039/b104468k.

[14] E.E.S. Teotonio, F.A. Silva, D.K.S. Pereira, L.M. Santo, H.F. Brito, W.M. Faustino, M.C.F.C. Felinto, R.H. Santos, R. Moreno-Fuquen, A.R. Kennedy, D. Gilmore, Luminescence enhancement of the Tb(III) ion with the thenoyltrifluoroacetonate ligand acting as an efficient sensitizer, Inorg. Chem. Commun. 13 (2010) 1391–1395. doi:10.1016/j.inoche.2010.07.043.

[15] F.A. Silva Jr., H.A. Nascimento, D.K.S. Pereira, E.E.S. Teotonio, H.F. Brito, M.C.F.C. Felinto, J.G.P. Espínola, G.F. Sá, W.M. Faustino, Energy Transfer Processes in Tb(III)-Dibenzoylmethanate Complexes with Phosphine Oxide Ligands, J. Braz. Chem. Soc. (2013). doi:10.5935/0103-5053.20130073.

[16] Y.C. Miranda, L.L.A.L. Pereira, J.H.P. Barbosa, H.F. Brito, M.C.F.C. Felinto, O.L. Malta, W.M. Faustino, E.E.S. Teotonio, The Role of the Ligand-to-Metal Charge-Transfer State in the Dipivaloylmethanate-Lanthanide Intramolecular Energy Transfer Process, Eur. J. Inorg. Chem. 2015 (2015) 3019–3027. doi:10.1002/ejic.201500263.

[17] R.O. Freire, G.B. Rocha, A.M. Simas, Sparkle/PM3 for the modeling of europium(III),

gadolinium(III), and terbium(III) complexes, J. Braz. Chem. Soc. 20 (2009) 1638–1645. doi:10.1590/S0103-50532009000900011.

[18] R.T. Moura Jr, A.N. Carneiro Neto, R.L. Longo, O.L. Malta, On the calculation and interpretation of covalency in the intensity parameters of 4f–4f transitions in Eu^{3+} complexes based on the chemical bond overlap polarizability, J. Lumin. 170 (2016) 420–430. doi:10.1016/j.jlumin.2015.08.016.

[19] O.L. Malta, A simple overlap model in lanthanide crystal-field theory, Chem. Phys. Lett. 87 (1982) 27–29. doi:10.1016/0009-2614(82)83546-X.

[20] A.N. Carneiro Neto, R.T. Moura, E.C. Aguiar, C. V Santos, M.A.F.L.B. de Medeiros, Theoretical study of geometric and spectroscopic properties of Eu(III) complexes with Ruhemann's Purple ligands, J. Lumin. 201 (2018) 451–459. doi:10.1016/j.jlumin.2018.05.014.

[21] I.P. Assunção, A.N. Carneiro Neto, R.T. Moura, C.C.S. Pedroso, I.G.N. Silva, M.C.F.C. Felinto, E.E.S. Teotonio, O.L. Malta, H.F. Brito, Odd-Even Effect on Luminescence Properties of Europium Aliphatic Dicarboxylate Complexes, ChemPhysChem. 20 (2019) 1931–1940. doi:10.1002/cphc.201900603.

[22] G.B.V. Lima, J.C. Bueno, A.F. da Silva, A.N. Carneiro Neto, R.T. Moura, E.E.S. Teotonio, O.L. Malta, W.M. Faustino, Novel trivalent europium β-diketonate complexes with N-(pyridine-2-yl)amides and N-(pyrimidine-2-yl)amides as ancillary ligands: Photophysical properties and theoretical structural modeling, J. Lumin. 219 (2020) 116884. doi:10.1016/j.jlumin.2019.116884.

[23] Rigaku Corporation, CrysAlisPRO, (2015).

[24] M.C. Burla, R. Caliandro, B. Carrozzini, G.L. Cascarano, C. Cuocci, C. Giacovazzo, M. Mallamo, A. Mazzone, G. Polidori, Crystal structure determination and refinement via SIR2014, J. Appl. Crystallogr. 48 (2015) 306–309. doi:10.1107/S1600576715001132.

[25] G.M. Sheldrick, Crystal structure refinement with SHELXL, Acta Crystallogr. Sect. C Struct. Chem. 71 (2015) 3–8. doi:10.1107/S2053229614024218.

[26] L.J. Farrugia, WinGX suite for small-molecule single-crystal crystallography, J. Appl. Crystallogr. 32 (1999) 837–838. doi:10.1107/S0021889899006020.

[27] L.J. Farrugia, ORTEP -3 for Windows - a version of ORTEP -III with a Graphical User Interface (GUI), J. Appl. Crystallogr. 30 (1997) 565–565. doi:10.1107/S0021889897003117.

[28] C.F. Macrae, I.J. Bruno, J.A. Chisholm, P.R. Edgington, P. McCabe, E. Pidcock, L. Rodriguez-Monge, R. Taylor, J. van de Streek, P.A. Wood, Mercury CSD 2.0 – new features for the visualization and investigation of crystal structures, J. Appl. Crystallogr. 41 (2008) 466–470. doi:10.1107/S0021889807067908.

[29] B. V. Bukvetskii, A.S. Shishov, A.G. Mirochnik, Triboluminescence and crystal structure of the centrosymmetric complex $[Tb(NO_3)_2(Acac)(Phen)_2]\cdot H_2O$, Luminescence. 31 (2016) 1329–1334. doi:10.1002/bio.3110.

[30] J.J.P. Stewart, MOPAC2016, (2016). http::://openmopac.net.

[31] A.D. Becke, A new mixing of Hartree–Fock and local density-functional theories, J. Chem. Phys. 98 (1993) 1372–1377. doi:10.1063/1.464304.

[32] C. Lee, W. Yang, R.G. Parr, Development of the Colle-Salvetti correlation-energy formula into a functional of the electron density, Phys. Rev. B. 37 (1988) 785–789. doi:10.1103/PhysRevB.37.785.

[33] S.H. Vosko, L. Wilk, M. Nusair, Accurate spin-dependent electron liquid correlation energies for local spin density calculations: a critical analysis, Can. J. Phys. 58 (1980) 1200–1211. doi:10.1139/p80-159.

[34] P.J. Stephens, F.J. Devlin, C.F. Chabalowski, M.J. Frisch, Ab Initio Calculation of Vibrational Absorption and Circular Dichroism Spectra Using Density Functional Force Fields, J. Phys. Chem. 98 (1994) 11623–11627. doi:10.1021/j100096a001.

[35] R.A. Kendall, T.H. Dunning, R.J. Harrison, Electron affinities of the first-row atoms revisited.

Systematic basis sets and wave functions, J. Chem. Phys. 96 (1992) 6796–6806. doi:10.1063/1.462569.

[36] M.W. Schmidt, K.K. Baldridge, J.A. Boatz, S.T. Elbert, M.S. Gordon, J.H. Jensen, S. Koseki, N. Matsunaga, K.A. Nguyen, S. Su, T.L. Windus, M. Dupuis, J.A. Montgomery Jr, General atomic and molecular electronic structure system, J. Comput. Chem. 14 (1993) 1347–1363. doi:10.1002/jcc.540141112.

[37] R.T. Moura Jr., A.N. Carneiro Neto, E.C. Aguiar, A. Shyichuk, R.L. Longo, E.E.S. Teotonio, W.M. Faustino, H.F. Brito, L.D. Carlos, O.L. Malta, JOYSpectra - Program for lanthanides luminescence calculations. Version 2019, (2019). http://www.cca.ufpb.br/gpqtc/joyspectra.

[38] Y.-Q. Zheng, L.-X. Zhou, J.-L. Lin, S.-W. Zhang, Syntheses and Crystal Structures of $Ln(phen)_2(NO_3)_3$ with Ln = Pr, Nd, Sm, Eu, Dy, and phen = 1,10-phenanthroline, Zeitschrift Für Anorg. Und Allg. Chemie. 627 (2001) 1643–1646. doi:10.1002/1521-3749(200107)627:7<1643::AID-ZAAC1643>3.0.CO;2-3.

[39] C. Wang, J. Kang, X. Zhang, Y. Zhao, H. Chu, Crystal structures and luminescence properties of lanthanide complexes with 4-bromobenzoate and nitrogen heterocyclic ligands, J. Lumin. 215 (2019) 116638. doi:10.1016/j.jlumin.2019.116638.

[40] H.F. Brito, O.M.L. Malta, M.C.F.C. Felinto, E.E.S. Teotonio, Luminescence Phenomena Involving Metal Enolates, in: PATAI'S Chem. Funct. Groups, John Wiley & Sons, Ltd, Chichester, UK, 2010. doi:10.1002/9780470682531.pat0419.

[41] A.N. Carneiro Neto, E.E.S. Teotonio, G.F. de Sá, H.F. Brito, J. Legendziewicz, L.D. Carlos, M.C.F.C. Felinto, P. Gawryszewska, R.T. Moura Jr., R.L. Longo, W.M. Faustino, O.L. Malta, Modeling intramolecular energy transfer in lanthanide chelates: A critical review and recent advances, in: Handb. Phys. Chem. Rare Earths, Vol. 56, Elsevier, 2019: pp. 55–162. doi:10.1016/bs.hpcre.2019.08.001.

[42] W.T. Carnall, H. Crosswhite, H.M. Crosswhite, Energy level structure and transition probabilities in the spectra of the trivalent lanthanides in LaF_3, Argonne, IL (United States), IL (United States), 1978. doi:10.2172/6417825.

[43] M.F. Reid, Theory of Rare-Earth Electronic Structure and Spectroscopy, in: Handb. Phys. Chem. Rare Earths, 1st ed., Elsevier B.V., 2016: pp. 47–64. doi:10.1016/bs.hpcre.2016.09.001.

[44] C. Görller-Walrand, K. Binnemans, Spectral intensities of f-f transitions, in: K.A. Gschneidner Jr., L. Eyring (Eds.), Handb. Phys. Chem. Rare Earths, Elsevier, 1998: pp. 101–264. doi:10.1016/S0168-1273(98)25006-9.

[45] B.R. Judd, Optical absorption intensities of rare-earth ions, Phys. Rev. 127 (1962) 750–761. doi:10.1103/PhysRev.127.750.

[46] G.S. Ofelt, Intensities of Crystal Spectra of Rare-Earth Ions, J. Chem. Phys. 37 (1962) 511–520. doi:10.1063/1.1701366.

[47] S.F. Mason, R.D. Peacock, B. Stewart, Ligand-polarization contributions to the intensity of hypersensitive trivalent lanthanide transitions, Mol. Phys. 30 (1975) 1829–1841.

[48] O.L. Malta, Theoretical crystal-field parameters for the $YOCl:Eu^{3+}$ system. A simple overlap model, Chem. Phys. Lett. 88 (1982) 353–356. doi:10.1016/0009-2614(82)87103-0.

[49] C.K. Jørgensen, B.R. Judd, Hypersensitive pseudoquadrupole transitions in lanthanides, Mol. Phys. 8 (1964) 281–290. doi:10.1080/00268976400100321.

[50] C.K. Jørgensen, R. Reisfeld, Judd-Ofelt parameters and chemical bonding, J. Less-Common Met. 93 (1983) 107–112. doi:10.1016/0022-5088(83)90454-X.

[51] J.D.L. Dutra, J.W. Ferreira, M.O. Rodrigues, R.O. Freire, Theoretical Methodologies for Calculation of Judd–Ofelt Intensity Parameters of Polyeuropium Systems, J. Phys. Chem. A. 117 (2013) 14095–14099. doi:10.1021/jp4098809.

[52] L. Smentek, Theoretical description of the spectroscopic properties of rare earth ions in crystals, Phys. Rep. 297 (1998) 155–237. doi:10.1016/S0370-1573(97)00077-X.

1

Highlights

- Europium(III) β-diketonate complexes were successfully synthesized.
- LMCT states play an essential role on the luminescent properties of Eu^{3+} complexes.
- The intensity parameters highly dependent on geometry and coordination number.

Experimental and theoretical investigations of the [Ln(β-dik)$(NO_3)_2(phen)_2]\cdot H_2O$ luminescent complexes

Paulo R. S. Santos[1], Dariston K. S. Pereira[1], Israel F. Costa[1], Iran F. Silva[1], Hermi F. Brito[2], Wagner M. Faustino[1], Albano N. Carneiro Neto[3], Renaldo T. Moura Jr.[4], Maria H. Araújo[5], Renata Diniz[5], Oscar L. Malta[6], Ercules E. S. Teotonio[1,*]

[1] Department of Chemistry, Federal University of Paraíba, João Pessoa, Brazil

[2] Institute of Chemistry, Department of Chemistry, University of São Paulo, São Paulo, Brazil

[3] Physics Department and CICECO – Aveiro Institute of Materials, University of Aveiro, Aveiro, Portugal

[4] Department of Chemistry and Physics, Federal University of Paraíba, Areia, Brazil

[5] Departament of Chemistry, ICEx, University of Minas Gerais, Belo Horizonte, MG 31270-901, Brazil

[6] Department of Fundamental Chemistry, Federal University of Pernambuco, Recife, Brazil

*Corresponding author: email: teotonioees@quimica.ufpb.br

Phone: +55-83-3216-7591

Author Statement

Paulo R. S. Santos and Israel F. Costa conceived, designed and performed the experiments; Paulo R. S. Santos and Iran F. Silva performed the measurement of spectroscopic data; Maria H. Araújo and Renata Diniz performed the structural resolution and revised the manuscript; Dariston K. S. Pereira, Albano N. Carneiro Neto and Renaldo T. Moura Jr. Performed the theoretical calculation and their analysis, and wrote the manuscript; Oscar L. Malta performed the theoretical and spectroscopic studies and revised the manuscript; Hermi F. Brito and Wagner M. Faustino performed analysis of spectroscopic data and revised the manuscript and Ercules E. S. Teotonio performed luminescence study and wrote the manuscript

Declaration of interests

☐ The authors declare that they have no known competing financial interests or personal relationships that could have appeared to influence the work reported in this paper.

☐The authors declare the following financial interests/personal relationships which may be considered as potential competing interests:

The authors declare that they have no known competing financial interests or personal relationships that could have appeared to influence the work reported in this paper